

QCD corrections to J/ψ polarization of hadronproduction at Tevatron and LHC

Bin Gong and Jian-Xiong Wang

*Institute of High Energy Physics, Chinese Academy of Sciences, P.O. Box 918(4), Beijing, 100049, China.
Theoretical Physics Center for Science Facilities, Beijing, 100049, China.*

(Dated: February 12, 2013)

The next to leading order (NLO) QCD corrections to J/ψ polarization of hadronproduction at Tevatron and LHC are calculated. The results show that the J/ψ polarization is extremely changed from more transversal polarization at leading order (LO) into more longitudinal polarization at NLO. Although it gives more longitudinal polarization than the recent experimental result on the J/ψ polarization at Tevatron. It sheds light on the solution to the large discrepancy of J/ψ polarization between theoretical predication and experimental measurement, and suggests that the next important step is to calculate the NLO correction for color octet state $J/\psi^{(8)}$ hadronproduction. Our calculations are performed in two ways where the polarizations are summed analytically or not, and they are checked with each other. It also gives a K factor for total cross section (ratio of NLO to LO) of about 2 and shows that the NLO corrections boost the J/ψ production for about 2 order of magnitude in high transverse momentum p_t region of J/ψ , which confirms the calculation by Campbell, Maltoni and Tramontano.

PACS numbers: 12.38.Bx, 13.25.Gv, 13.60.Le

The study of J/ψ production on various experiments is a very interesting topic since its discovery in 1974. It is a good place to probe both perturbative and nonperturbative aspects of QCD dynamics. To describe the huge discrepancy of the high- p_t J/ψ production between the theoretical calculation and the experimental measurement, color-octet mechanism[1] was proposed based on the non-relativistic QCD(NRQCD)[2]. The factorization formalism of NRQCD provides a theoretical framework to the treatment of heavy-quarkonium production. It allows consistent theoretical prediction to be made and to be improved perturbatively in the QCD coupling constant α_s and the heavy-quark relative velocity v . Although it seems to show qualitative agreements with experimental data, there are certain difficulties in the quantitative estimate in NRQCD for J/ψ and ψ' photoproduction at the DESY ep collider HERA [3, 4], $J/\psi(\psi')$ polarization of hadronproduction at the Fermilab Tevatron, and J/ψ production in B-factories.

There are a few examples shown that NLO corrections are quite large and it is difficult to obtain agreement between the experimental results and leading order theoretical predictions for J/ψ production. It was found that the current experimental results on inelastic J/ψ photoproduction are adequately described by the color singlet channel alone once higher-order QCD corrections are included[4]. Ref. [5] found that the DELPHI [6] data evidently favor the NRQCD formalism for J/ψ production $\gamma\gamma \rightarrow J/\psi X$, but rather the color-singlet mechanism. And it was also found in ref. [7] that the QCD higher order process $\gamma\gamma \rightarrow J/\psi c\bar{c}$ gives the same order and even larger contribution at high p_t than the leading order color singlet processes. In ref. [8], at NLO the process $c\bar{g} \rightarrow J/\psi c$ where the initial c quark is the intrinsic c quark from proton at Tevatron, gives larger contribution at high p_t than the leading order color singlet processes. The large discrepancies found in the single and double

charmonium production in e^+e^- annihilation at B factories between LO theoretical predictions [9, 10] and experimental results [11, 12] were studied in many work. It seems that it may be resolved by including higher order correction: NLO QCD and relativistic corrections [9, 13, 14].

Based on NRQCD, the LO calculation predicts a sizable transverse polarization for J/ψ at high p_t [15] while the measurement at Fermilab Tevatron[16] gives almost unpolarized result. Recently, NLO QCD corrections to J/ψ hadronproduction have been calculated by Campbell, Maltoni and Tramontano[17]. The results show that the total cross section is boosted by a factor of about 2 and the J/ψ transverse momentum p_t distribution is enhanced more and more as p_t becomes larger. A real correction process $g\bar{g} \rightarrow J/\psi c\bar{c}$ at NLO was calculated by Artoisenet, Lansberg and Maltoni[18]. It gives sizable contribution to p_t distribution of J/ψ at high p_t region, and it alone gives almost unpolarized result. A s-channel treatment to J/ψ hadronproduction gives longitudinal polarization by H. Habermann and J. P. Lansberg[19]. Therefore it is very interesting to know the result of J/ψ polarization when NLO QCD corrections are included. In this letter, we calculate the NLO QCD corrections to the J/ψ polarization in hadronproduction at Tevatron and LHC. In the calculation, we use our Feynman Diagram Calculation package (FDC)[20] with newly added part of a complete set of method to calculate tensor and scalar integrals in dimensional regularization, which was used in our previous work[14].

For LO process $g(p_1) + g(p_2) \rightarrow J/\psi(p_3) + g(p_4)$, by using the NRQCD factorization formalism, the partonic cross section is expressed as

$$\frac{d\hat{\sigma}^B}{dt} = \frac{5\pi\alpha_s^3 |R_s(0)|^2 [s^2(s-1)^2 + t^2(t-1)^2 + u^2(u-1)^2]}{144m_c^5 s^2(s-1)^2(t-1)^2(u-1)^2}, \quad (1)$$

with

$$s = \frac{(p_1 + p_2)^2}{4m_c^2}, \quad t = \frac{(p_1 - p_3)^2}{4m_c^2}, \quad u = \frac{(p_1 - p_4)^2}{4m_c^2},$$

where $R_s(0)$ is the radial wave function at the origin of J/ψ and the approximation $M_{J/\psi} = 2m_c$ is taken. The LO total cross section is obtained by convoluting the partonic cross section with the parton distribution function (PDF) $G_g(x, \mu_f)$ in the proton:

$$\sigma^B = \int dx_1 dx_2 G_g(x_1, \mu_f) G_g(x_2, \mu_f) \hat{\sigma}^B, \quad (2)$$

where μ_f is the factorization scale. In the following, $\hat{\sigma}$ represents corresponding partonic cross section.

The NLO contribution to the process can be separated into the virtual corrections, arising from loop diagrams, and the real corrections, arising from the radiation of a real gluon or a light (anti)quark or the final-state gluon splits into light quark-antiquark pairs. There are UV, IR and Coulomb singularities in the calculation of the virtual corrections. UV-divergences from self-energy and triangle diagrams are canceled upon the renormalization of the QCD gauge coupling constant, the charm quark mass and field, and the gluon field. Here we adopt same renormalization scheme as ref. [21]. The renormalization constant of charm quark mass Z_m and field Z_2 , and gluon field Z_3 are defined in the on-mass-shell(OS) scheme while that of QCD gauge coupling Z_g is defined in the modified-minimal-subtraction($\overline{\text{MS}}$) scheme:

$$\begin{aligned} \delta Z_m^{OS} &= -3C_F \frac{\alpha_s}{4\pi} \left[\frac{1}{\epsilon_{UV}} - \gamma_E + \ln \frac{4\pi\mu_r^2}{m_c^2} + \frac{4}{3} \right], \\ \delta Z_2^{OS} &= -C_F \frac{\alpha_s}{4\pi} \left[\frac{1}{\epsilon_{UV}} + \frac{2}{\epsilon_{IR}} - 3\gamma_E + 3 \ln \frac{4\pi\mu_r^2}{m_c^2} + 4 \right], \\ \delta Z_3^{OS} &= \frac{\alpha_s}{4\pi} \left[(\beta_0 - 2C_A) \left(\frac{1}{\epsilon_{UV}} - \frac{1}{\epsilon_{IR}} \right) \right], \\ \delta Z_g^{\overline{\text{MS}}} &= -\frac{\beta_0}{2} \frac{\alpha_s}{4\pi} \left[\frac{1}{\epsilon_{UV}} - \gamma_E + \ln(4\pi) \right]. \end{aligned} \quad (3)$$

Where γ_E is Euler's constant, $\beta_0 = \frac{11}{3}C_A - \frac{4}{3}T_F n_f$ is the one-loop coefficient of the QCD beta function and n_f is the number of active quark flavors. There are three massless light quarks u, d, s , so $n_f=3$. In $SU(3)_c$, color factors are given by $T_F = \frac{1}{2}$, $C_F = \frac{4}{3}$, $C_A = 3$. And μ_r is the renormalization scale.

After having fixed the renormalization scheme, there are 129 NLO diagrams, including counter-term diagrams, which are shown in Fig. 1, divided into 8 groups. Diagrams of group (e) that has a virtual gluon line connected with the quark pair lead to Coulomb singularity $\sim \pi^2/v$, which can be isolated by introducing a small relative velocity $v = |\vec{p}_c - \vec{p}_{\bar{c}}|$ and mapped into the $c\bar{c}$ wave function. By adding all diagrams together, the virtual corrections to the differential cross section can be connected to the virtual amplitude as

$$\frac{d\hat{\sigma}^V}{dt} \propto 2\text{Re}(M^B M^{V*}), \quad (4)$$

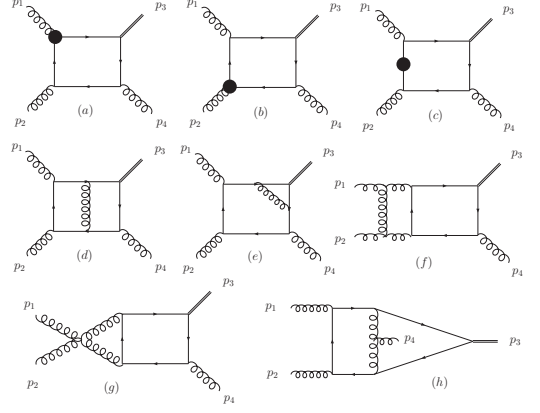


FIG. 1: One-loop diagrams for $gg \rightarrow J/\psi g$. Group (a) and (b) are counter-term diagrams of the quark-gluon vertex and corresponding loop diagrams, Group (c) are the quark self-energy diagrams and corresponding counter-term ones. More diagrams can be obtained by permutation of external gluons.

where M^B is the amplitude at LO, and M^V is the renormalized amplitude at NLO and is UV and Coulomb finite, but it still contains the IR divergences:

$$\begin{aligned} M^V|_{IR} &= \frac{\alpha_s}{2\pi} \frac{\Gamma(1-\epsilon)}{\Gamma(1-2\epsilon)} \left(\frac{4\pi\mu_r^2}{s_{12}} \right)^\epsilon \left[-\frac{9}{2\epsilon^2} - \frac{3}{2\epsilon} \right. \\ &\quad \left. \times \left(\ln \frac{s}{-t} + \ln \frac{s}{-u} - \frac{1}{3}n_f + \frac{11}{2} \right) \right] M^B. \end{aligned} \quad (5)$$

The real corrections arise from processes $gg \rightarrow J/\psi gg$, $gg \rightarrow J/\psi q\bar{q}$ and $gq(\bar{q}) \rightarrow J/\psi gq(\bar{q})$. The phase space integration of above processes will generate IR singularities, which are either soft or collinear and can be conveniently isolated by slicing the phase space into different regions. We use the two-cutoff phase space slicing method [22], which introduces two small cutoffs to decompose the phase space into three parts. And then the real cross section could be written as

$$\sigma^R = \sigma^{H\overline{C}} + \sigma^S + \sigma^{HC} + \sigma_{add}^{HC}. \quad (6)$$

The hard noncollinear part $\sigma^{H\overline{C}}$ is IR finite and is numerically computed using standard Monte-Carlo integration techniques. $\hat{\sigma}^S$ from the soft regions contains soft singularities and is calculated analytically under soft approximation. It is easy to find that soft singularities for a gluon emitted from the charm quark pair in the S-wave color singlet J/ψ are canceled by each other. σ^{HC} from the hard collinear regions contains collinear singularities which is factorized and partly absorbed into the redefinition of the PDF (usually called mass factorization [23]). Here we adopt a scale dependent PDF using the $\overline{\text{MS}}$ convention given by [22]. After the redefinition of the PDF, an additional term σ_{add}^{HC} is separated out. Finally, all the IR singularities are canceled analytically for $\hat{\sigma}^S + \hat{\sigma}^{HC} + \hat{\sigma}^V$. And it is found that only one color factor d_{abc} appears in both M^B and M^V with a, b and c being the color index of the three gluons in the process.

To obtain the transverse momentum distribution of J/ψ , a transformation for integration variables ($dx_2 dt \rightarrow J dp_t dy$) is introduced. Thus we have

$$\frac{d\sigma}{dp_t} = \int J dx_1 dy G_g(x_1, \mu_f) G_g(x_2, \mu_f) \frac{d\hat{\sigma}}{dt}, \quad (7)$$

where y and p_t is the rapidity and transverse momentum of J/ψ in laboratory frame respectively. The polarization measurement α is defined as:

$$\alpha(p_t) = \frac{d\sigma_T/dp_t - 2d\sigma_L/dp_t}{d\sigma_T/dp_t + 2d\sigma_L/dp_t}. \quad (8)$$

It represents the measurement of J/ψ polarization as function of p_t . To calculate $\alpha(p_t)$, the polarization of J/ψ must be kept in the calculation. The partonic differential cross section with J/ψ polarized could be expressed explicitly as:

$$\frac{d\hat{\sigma}_\lambda}{dt} = a \epsilon(\lambda) \cdot \epsilon^*(\lambda) + \sum_{i,j=1,2} a_{ij} p_i \cdot \epsilon(\lambda) p_j \cdot \epsilon^*(\lambda), \quad (9)$$

where $\lambda = T_1, T_2, L$. $\epsilon(T_1)$, $\epsilon(T_2)$, $\epsilon(L)$ are the two transverse polarization vectors and the longitude one for J/ψ , and the polarization of all the other particles are summed up in n-dimensions. It causes more difficult tensor reduction path than that with all the polarization being summed over in virtual correction calculation. It is founded that a and a_{ij} are finite when the virtual correction and real correction are summed up.

For σ_{add}^{HC} and $\hat{\sigma}^S + \hat{\sigma}^{HC} + \hat{\sigma}^V$, the calculation is done in Eq. (9) as well as in the usual way in which the polarization for all particles are summed up. The two results are used to check with each other numerically. In the third way, the polarization of gluon is also kept and used to check gauge invariance by replacing the gluon polarization vector to the gluon's 4-momentum in the final numerical calculation. To calculate σ^{HC} in real correction processes, the numerical amplitude calculation is used and the polarization of gluons are only summed for their physical freedom to avoid the involving of diagrams with external ghosts lines.

In our numerical calculations, the CTEQ6L1 and CTEQ6M PDFs, and the corresponding fitted value for $\alpha_s(M_Z) = 0.130$ and $\alpha_s(M_Z) = 0.118$, are used for LO and NLO predictions respectively. For the charm quark mass and the wave function at the origin of J/ψ , $m_c = 1.5$ GeV and $|R_s(0)|^2 = 0.810$ GeV³ are used. The two phase space cutoffs δ_s and δ_c are chosen as $\delta_s = 10^{-3}$ and $\delta_c = \delta_s/50$ as default choice. To check the two cutoffs invariance for the final results, different values of δ_s and δ_c , down to $\delta_s = 10^{-5}$, are used and the invariance is found within the error control (less than one percent). It is known that the perturbative expansion calculation is not applicable to the regions with small transverse momentum and large rapidity of J/ψ . Therefore, the result is restricted in the domain $p_t > 3$ GeV and $|y_{J/\psi}|$ less than 3 or 0.6.

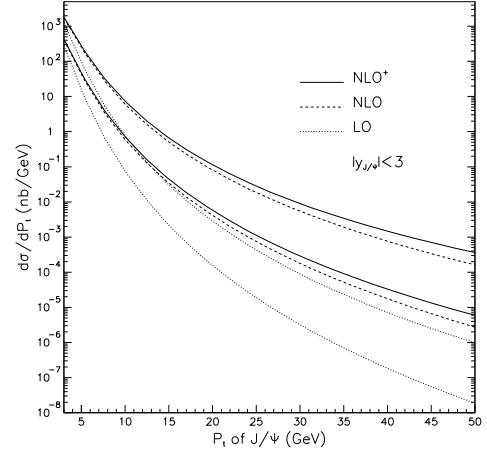


FIG. 2: Transverse momentum distribution of differential cross section with $\mu_r = \mu_f = \sqrt{(2m_c)^2 + p_t^2}$ at LHC (upper curves) and Tevatron (lower curves). Center mass energy are $\sqrt{s}_{\text{Tevatron}} = 1.98$ TeV and $\sqrt{s}_{\text{LHC}} = 14$ TeV. NLO⁺ denotes result including contribution from $gg \rightarrow J/\psi c\bar{c}$ at NLO.

The dependence of the total cross section at the renormalization scale μ_r and factorization scale μ_f are obtained and it agrees with the Fig.3 in ref [17]. In Fig. 2, the p_t distribution of J/ψ is shown. The p_t distribution of J/ψ polarization α is shown in Fig. 3. At LO, α is always positive and becomes closer to 1 as p_t increases from 3 GeV to 50 GeV, which indicates that transverse polarization is always larger than longitude polarization and transverse polarization plays the major role in high p_t region. But there is extremely change when including NLO QCD corrections. α is always negative and becomes closer to -0.9 as p_t increases from 3 GeV to 50 GeV, which indicates that transverse polarization is always smaller than longitude polarization and longitude polarization plays the major role in high p_t region. Meanwhile the J/ψ polarization of process $gg \rightarrow J/\psi c\bar{c}$ is near zero. By including contribution of this subprocess, the result shown in the figures as NLO⁺ is closer to the experimental result.

In conclusion, we calculated the NLO QCD correction of J/ψ hadronproduction at Tevatron and LHC. The method of dimensional regularization is taken to deal with the UV and IR singularities in the calculation, and the Coulomb singularity is isolated and absorbed into the $c\bar{c}$ bound state wave function. To deal with the soft and collinear singularities, the two-cutoff phase space slicing method is used in the calculation of real corrections. After adding all contribution together, a result which is UV, IR and Coulomb finite is obtained. Numerically, we obtain a K factor of total cross section (ratio of NLO to LO) of about 2 at $\mu_r = \mu_f = \sqrt{(2m_c)^2 + p_t^2}$. The transverse momentum distribution of J/ψ is presented and it shows that the NLO corrections would boost the differential cross section more and more as p_t becomes larger and reaches about 2 or 3 order of magnitude at $p_t = 50$ GeV. It confirms the calculation in Ref. [17].

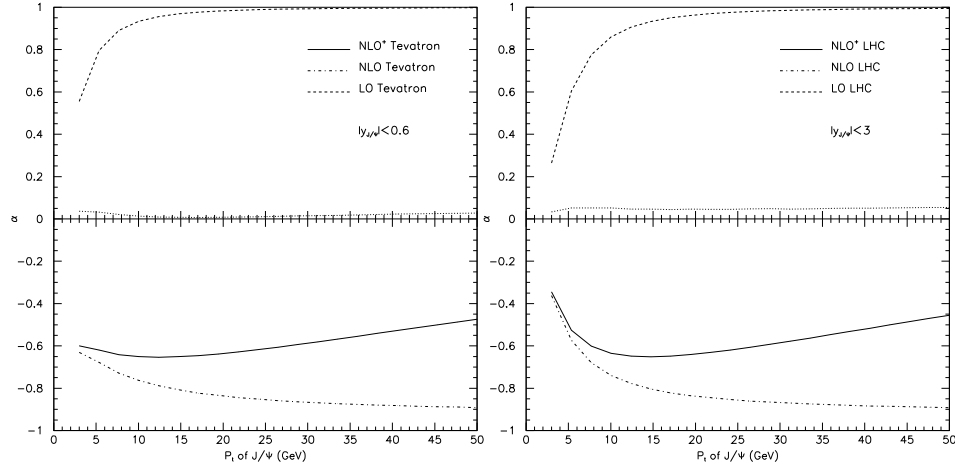


FIG. 3: Transverse momentum distribution of polarization α with $\mu_r = \mu_f = \sqrt{(2m_c)^2 + p_t^2}$ at Tevatron(left) and LHC(right). The unlabeled dotted line denotes the polarization of $gg \rightarrow J/\psi c\bar{c}$ and NLO⁺ denotes result including that of $gg \rightarrow J/\psi c\bar{c}$.

The real corrections for $gg \rightarrow J/\psi c\bar{c}$ is also calculated and agree with those of Ref. [18].

The J/ψ polarization at NLO is studied for the first time and the results show that the J/ψ polarization is extremely changed from more transversal polarization at LO into more longitudinal polarization at NLO. Although it gives more longitudinal polarization than the recent experimental result [16] on the J/ψ polarization at Tevatron. It sheds light on the solution to the large discrepancy of J/ψ polarization between LO theoretical

prediction and the experimental measurement, and suggests that the next important step is to calculate the NLO correction for color octet state $J/\psi^{(8)}$ hadronproduction. To re-fix the color-octet matrix elements and to see what happens to the polarization of J/ψ at NLO.

This work is supported by the National Natural Science Foundation of China (No. 10775141) and by the Chinese Academy of Sciences under Project No. KJCX3-SYW-N2.

-
- [1] E. Braaten and S. Fleming, Phys. Rev. Lett. **74**, 3327 (1995).
 - [2] G. T. Bodwin, E. Braaten, and G. P. Lepage, Phys. Rev. **D51**, 1125 (1995).
 - [3] P. Ko, J. Lee and H. S. Song, Phys. Rev. **D54**, 4312 (1996); B. A. Kniehl and G. Kramer, Phys. Lett. **B413**, 416 (1997).
 - [4] M. Kramer Nucl. Phys. **B459**, 3 (1996); M. Kramer, J. Zunft, J. Steegborn and P. M. Zerwas, Phys. Lett. **B348**, 657 (1995); M. Cacciari and M. Kramer, Phys. Rev. Lett. **76**, 4128 (1996); J. Amundson, S. Fleming and I. Maksymyk, Phys. Rev. **D56**, 5844 (1997).
 - [5] M. Klasen, B. A. Kniehl, L. N. Mihaila, and M. Steinhauser, Phys. Rev. Lett. **89**, 032001 (2002).
 - [6] W. de Boer and C. Sander, Phys. Lett. **B585**, 276 (2004).
 - [7] C. F. Qiao and J. X. Wang, Phys. Rev. **D69**, 014015 (2004).
 - [8] K. Hagiwara, W. Qi, C. F. Qiao, and J. X. Wang (2007), arXiv:0705.0803 [hep-ph].
 - [9] E. Braaten and J. Lee, Phys. Rev. **D67**, 054007 (2003).
 - [10] K.-Y. Liu, Z.-G. He and K.-T. Chao, Phys. Lett. **B557**, 45 (2003); K. Hagiwara, E. Kou and C.-F. Qiao, Phys. Lett. **B570**, 39 (2003).
 - [11] K. Abe et al. (Belle), Phys. Rev. Lett. **89**, 142001 (2002).
 - [12] B. Aubert et al. (BABAR), Phys. Rev. **D72**, 031101 (2005).
 - [13] Y.-J. Zhang, Y.-j. Gao and K.-T. Chao, Phys. Rev. Lett. **96**, 092001 (2006). Z.-G. He, Y. Fan and K.-T. Chao, Phys. Rev. **D75**, 074011 (2007). Y.-J. Zhang and K.-T. Chao, Phys. Rev. Lett. **98**, 092003 (2007).
 - [14] B. Gong and J.-X. Wang, arXiv:0712.4220 [hep-ph], (2007); arXiv:0801.0648 [hep-ph], (2008)
 - [15] M. Beneke and I.Z. Rothstein, Phys. Lett. **B372**, 157 (1996), [Erratum-ibid. **B389**, 769 (1996)]; M. Beneke and M. Krämer, Phys. Rev. **D55**, 5269 (1997). E. Braaten, B.A. Kniehl, and J. Lee, Phys. Rev. **D62**, 094005 (2000); B. A. Kniehl and J. Lee, Phys. Rev. **D62**, 114027 (2000). A. K. Leibovich, Phys. Rev. Dbf 56, 4412 (1997).
 - [16] A. Abulencia et al. (CDF), Phys. Rev. Lett. **99**, 132001 (2007).
 - [17] J. Campbell, F. Maltoni, and F. Tramontano, Phys. Rev. Lett. **98**, 252002 (2007).
 - [18] P. Artoisenet, J. P. Lansberg, and F. Maltoni, Phys. Lett. **B653**, 60 (2007).
 - [19] H. Haberzettl and J. P. Lansberg, Phys. Rev. Lett. **100**, 032006 (2008)
 - [20] J.-X. Wang, Nucl. Instrum. Meth. **A534**, 241 (2004).
 - [21] M. Klasen, B. A. Kniehl, L. N. Mihaila, and M. Steinhauser, Nucl. Phys. **B713**, 487 (2005).
 - [22] B. W. Harris and J. F. Owens, Phys. Rev. **D65**, 094032 (2002).
 - [23] G. Altarelli, R. K. Ellis, and G. Martinelli, Nucl. Phys. **B157**, 461 (1979).